www.nature.com/aps

Acta Pharmacologica Sinica

ARTICLE

Cardamonin protects against lipopolysaccharide-induced myocardial contractile dysfunction in mice through Nrf2-regulated mechanism

Ying Tan[1,2,3], Hong-hong Wan[4], Ming-ming Sun[3], Wen-jing Zhang[4], Maolong Dong[1,2,3], Wei Ge[3,5], Jun Ren[3] and Hu Peng[4]

In patients with sepsis, lipopolysaccharide (LPS) from the outer membrane of gram-negative bacteria triggers cardiac dysfunction and heart failure, but target therapy for septic cardiomyopathy remains unavailable. In this study we evaluated the beneficial effects of cardamonin (CAR), a flavone existing in Alpinia plant, on endotoxemia-induced cardiac dysfunction and the underlying mechanisms with focus on oxidative stress and apoptosis. Adult mice were exposed to LPS (4 mg/kg, i.p. for 6 h) prior to functional or biochemical assessments. CAR (20 mg/kg, p.o.) was administered to mice immediately prior to LPS challenge. We found that LPS challenge compromised cardiac contractile function, evidenced by compromised fractional shortening, peak shortening, maximal velocity of shortening/relengthening, enlarged LV end systolic diameter and prolonged relengthening in echocardiography, and induced apoptosis, overt oxidative stress (O_2^- production and reduced antioxidant defense) associated with inflammation, phosphorylation of NF-κB and cytosolic translocation of transcriptional factor Nrf2. These deteriorative effects were greatly attenuated or mitigated by CAR administration. However, H&E and Masson's trichrome staining analysis revealed that neither LPS challenge nor CAR administration significantly affected cardiomyocyte cross-sectional area and interstitial fibrosis. Mouse cardiomyocytes were treated with LPS (4 μg/mL) for 6 h in the absence or presence of CAR (10 μM) in vitro. We found that addition of CAR suppressed LPS-induced defect in cardiomyocyte shortening, which was nullified by the Nrf2 inhibitor ML-385 or the NF-κB activator prostratin. Taken together, our results suggest that CAR administration protects against LPS-induced cardiac contractile abnormality, oxidative stress, apoptosis, and inflammation through Nrf2- and NF-κB-dependent mechanism.

Keywords: cardamonin; lipopolysaccharide; cardiac dysfunction; inflammation; apoptosis; oxidative stress

Acta Pharmacologica Sinica (2021) 42:404–413; https://doi.org/10.1038/s41401-020-0397-3

INTRODUCTION

Sepsis is a life-threatening medical emergency triggered by organismal infection and compromised organ defense against infection. Severe multiorgan injury is commonly observed in sepsis, including cardiac geometric and contractile dysfunction, which manifests as dilated heart chambers, impaired contractility, and reduced cardiac output [1–4]. It is well known that septic cardiomyopathy overtly increases overall mortality in hospitalized patients with sepsis, regardless of any preexisting cardiovascular anomalies [5, 6]. Even with the modern medical technology and clinical management for sepsis [7, 8], effective targeted therapy against septic cardiomyopathy remains rather challenging.

ONE of the hallmarks of sepsis is the onset and development of the inflammatory response, characterized by a profound elevation in a cadre of inflammatory cytokines that contribute to the pathogenesis of cardiac anomalies in sepsis [9]. Earlier findings from our lab and other groups have indicated a cardinal role for lipopolysaccharide (LPS) originating from gram-negative bacteria in cardiac dysfunction in sepsis. In particular, cardiomyocytes serve as targets for apoptosis as a result of excess inflammation [10]. With excess inflammatory mediators and microbial products surrounding cardiomyocytes in sepsis, large numbers of reactive oxygen and nitrogen species, superoxide anion (O_2^-), and nitric oxide are generated, resulting in amplified inflammatory reactions and tissue damage in the heart [11, 12]. A number of antioxidants (such as metallothionein, catalase, and insulin-like growth factor I) along with mitochondrial aldehyde dehydrogenase (ALDH2) have been shown to have promise in the management of cardiac dysfunction in sepsis [2, 3, 10, 13], although clinical validation is still lacking for antioxidants in sepsis and septic hearts.

Flavonoids possess a wide array of biological properties encompassing free radical scavenging and anti-inflammation to alleviate the overall risks of cardiovascular diseases [14–16]. Cardamonin (CAR), a flavone compound naturally residing in multiple herbs, such as *Alpinia katsumadai*, *Ginkgo biloba*, and *Carya cathayensis* Sarg, has various pharmacological properties,

[1]Department of Emergency Medicine, Nanfang Hospital, Southern Medical University, Guangzhou 510515, China; [2]Department of Burns, Nanfang Hospital, Southern Medical University, Guangzhou 510515, China; [3]Center for Cardiovascular Research and Alternative Medicine, University of Wyoming College of Health Sciences, Laramie, WY 82071, USA; [4]Department of Emergency, Shanghai Tenth People's Hospital, Tongji University School of Medicine, Shanghai 200072, China and [5]Department of General Practice, Xijing Hospital, the Air Force Military Medical University, Xi'an 710032, China
Correspondence: Maolong Dong (2206723777@qq.com) or Wei Ge (geweidr@fmmu.edu.cn) or Jun Ren (jren@uwyo.edu) or Hu Peng (1973denkepeng@tongji.edu.cn)
These authors contributed equally: Ying Tan, Hong-hong Wan, Ming-ming Sun

Received: 15 November 2019 Accepted: 15 March 2020
Published online: 21 April 2020

including antitumor, antioxidant, anti-inflammatory, and anticoagulative activities [17–19]. The beneficial effect of CAR has been documented in sepsis and cardiovascular anomalies. In a murine model of sepsis, CAR was shown to protect against acute septic lung injury through suppression of systemic inflammatory responses by downregulating tumor necrosis factor-α (TNF-α) and interleukins (e.g., IL-1β and IL-6) [20]. Wang et al. reported that CAR inhibited the activation of the NOD-, LRR-, and pyrin domain-containing protein 3 (NLRP3) inflammasome in macrophages and monocytes as well as retarded NLRP3-associated septic shock [21]. In addition, CAR was found to retard pressure overload-induced cardiac anomalies through antagonism of oxidative stress [22]. Khaizurin et al. further confirmed that CAR is capable of downregulating inducible nitric oxide synthase (iNOS) through inhibition of p65/nuclear factor-κB (NF-κB) nuclear translocation and IκBα phosphorylation [23]. Activation of NF-κB by LPS and cytokines has been shown to provoke redox balance. Thus, it is likely that CAR exerts its beneficial cardiovascular effects through the regulation of redox balance [24]. These findings suggest that CAR might offer protective effects on sepsis and septic cardiomyopathy. To this end, this study was designed to examine the possible effect of CAR on septic cardiomyopathy experimentally induced by LPS and the mechanism involved. Given the pivotal role of oxidative stress and inflammation in septic hearts [25–27], the levels of O_2^-, antioxidant enzymes, apoptosis, and proinflammatory markers were monitored. The levels of the essential redox regulating signals nuclear factor erythroid 2-like 2 (Nrf2) and NF-κB were evaluated in murine hearts.

MATERIALS AND METHODS

LPS challenge and CAR treatment

All animal procedures were approved by the Animal Care and Use Committees at the Shanghai Tenth People's Hospital, Tongji University (Shanghai, China) and the Southern Medical University (Guangzhou, China) and were in compliance with the NIH Guide for the Care and Use of Laboratory Animals. In brief, 4- to 5-month-old adult C57 mice (both genders) were kept in climate-controlled cages (22.8 ± 2.0 °C) with a 12/12-h light/dark cycle. Mice were allowed ad libitum access to food and water. Mice were challenged with 4 mg/kg *Escherichia coli* O55:B5 LPS dissolved in saline intraperitoneally and were then maintained in temperature-controlled cages for 6 h prior to functional or biochemical assessments [4]. The choice of 6 h for LPS was made according to established protocols from our lab and others [13, 25, 28, 29]. Cohorts of mice received CAR treatment (20 mg/kg, p.o.) immediately prior to LPS challenge or saline.

Echocardiographic assessment

Cardiac function was assessed in anesthetized (ketamine 80 mg/kg and xylazine 12 mg/kg, i.p.) mice using M-mode echocardiography (Vevo 2100, FUJIFILM Visualsonics, Toronto, ON, Canada) equipped with a 22–55 MHz transducer (MS550D, FUJIFILM VisualSonics). Hearts were imaged in 2-D mode in the parasternal long-axis view prior to M-mode imaging positioned perpendicular to the interventricular septum and posterior left ventricular (LV) wall. LV wall thickness and LV end diastolic and end systolic dimensions (EDD and ESD) were recorded, and fractional shortening was calculated using the equation [(EDD-ESD)/EDD] × 100. Heart rate was measured over 10 consecutive cycles [30].

Histopathological analysis and terminal deoxynucleotidyl transferase dUTP nick end labeling (TUNEL) staining

Hearts were removed and arrested in diastolic phase using KCl prior to fixation in 10% formalin overnight. The samples were dehydrated using graded alcohols, cleared in xylenes, and embedded in paraffin. Serial sections were then cut into 5-μm thick sections prior to H&E staining [30]. Masson's trichrome staining was employed to assess tissue fibrosis. The percentage of the light blue-stained area normalized to the entire area was considered an indicator of fibrosis. TUNEL staining was performed to assess apoptosis [31].

Isolation of cardiomyocytes and in vitro drug treatment

Isolated hearts were perfused with a modified Tyrode solution via a thermostat (37 °C) Langendorff system (AD Instruments, Colorado Spring, CO, USA) prior to exposure to Liberase Blendzyme 4. Following digestion, left ventricles were cut and minced into small pieces prior to resuspension [32]. The cardiomyocyte yield was ~70% and was unaffected by CAR or LPS. To evaluate the roles of Nrf2 and NFκB in LPS-induced cardiomyocyte anomalies, cardiomyocytes from C57 mice were challenged with LPS (4 μg/mL) [2] for 6 h in the absence or presence of CAR (10 μM) [21], the Nrf2 inhibitor ML-385 (20 μM) [33], or the NF-κB activator prostratin (2 μM) [34] before mechanical evaluation.

Cell shortening/relengthening

The contractile properties of cardiomyocytes were evaluated using a SoftEdge Myocam (IonOptix, Milton, MA, USA). In brief, cells were loaded onto a chamber mounted on the stage of an inverted microscope (Olympus IX-70) and were perfused (~2 ml/min at 25 °C) with Krebs–Henseleit bicarbonate buffer containing 1 mM $CaCl_2$. Cells were field stimulated at a frequency of 0.5 Hz. Cell shortening was recorded, including peak shortening (PS), time-to-PS (TPS), time-to-90% relengthening (TR_{90}), and the maximal velocities of shortening/relengthening ($\pm dL/dt$) [32].

Superoxide (O_2^-)

Intracellular O_2^- was evaluated using fluorescence probe oxidation. In brief, cardiomyocytes were loaded with dihydroethidium (DHE) (5 μM, Molecular Probes, Eugene, OR, USA) prior to assessment using an Olympus BX-51 microscope with an Olympus MagnaFire™ SP digital camera. Fluorescence was quantitated using a fluorescent microplate reader at an excitation wavelength of 480 nm and an emission wavelength of 530 nm [35, 36].

Western blot analysis

Tissue homogenates were resolved using SDS-polyacrylamide gels, and proteins were transferred onto nitrocellulose membranes prior to an overnight incubation with primary antibodies at 4 °C. The membranes were treated with a horseradish peroxidase-coupled secondary antibody, and the density was measured using a Bio-Rad calibrated densitometer. To reprobe the loading control GAPDH, membranes were stripped with 50 mM Tris-HCl, 2% SDS, and 0.1 M β-mercaptoethanol. The following antibodies were used for immunoblotting: IL-1β [Santa Cruz Biotechnology (SCBT), Santa Cruz, CA, USA, catalog# sc-7884], Bax (Cell Signaling, Danvers, MA, USA, catalog# 2772), Bcl-2 (Cell Signaling, catalog# 2876S), Caspase-3 (Cell Signaling, catalog# 9662), cleaved Caspase-3 (SCBT, catalog# sc-7272), SOD1 (Cell Signaling, catalog# 4266), Nrf2 (Cell Signaling, catalog# 12721), Catalase (Cell Signaling, catalog# 14097), TNF-α (Cell Signaling, catalog# 3707), IL-6 (Cell Signaling, catalog# 12912), and GAPDH (Cell Signaling, catalog# 2118L) [25].

qRT-PCR

Total RNA was extracted using TRIzol reagent. RNA was reverse transcribed into complementary DNA using stem-loop reverse transcription primers [37]. First-strand mRNAs were produced using a HiScript II Q RT SuperMix for qPCR (Vazyme Biotech Co, Ltd), and quantitative real-time PCR analysis (qRT-PCR) was conducted using ChamQTM Universal SYBR qPCR Master Mix (Vazyme Biotech Co., Ltd) on a Bio-Rad CFX96TM Real-Time PCR machine (Bio-Rad) [38]. The levels of genes were quantified using the comparative ΔΔCt method with normalization to MeEF1a. The Vazyme cycling conditions were 95 °C for 30 s, followed by 39

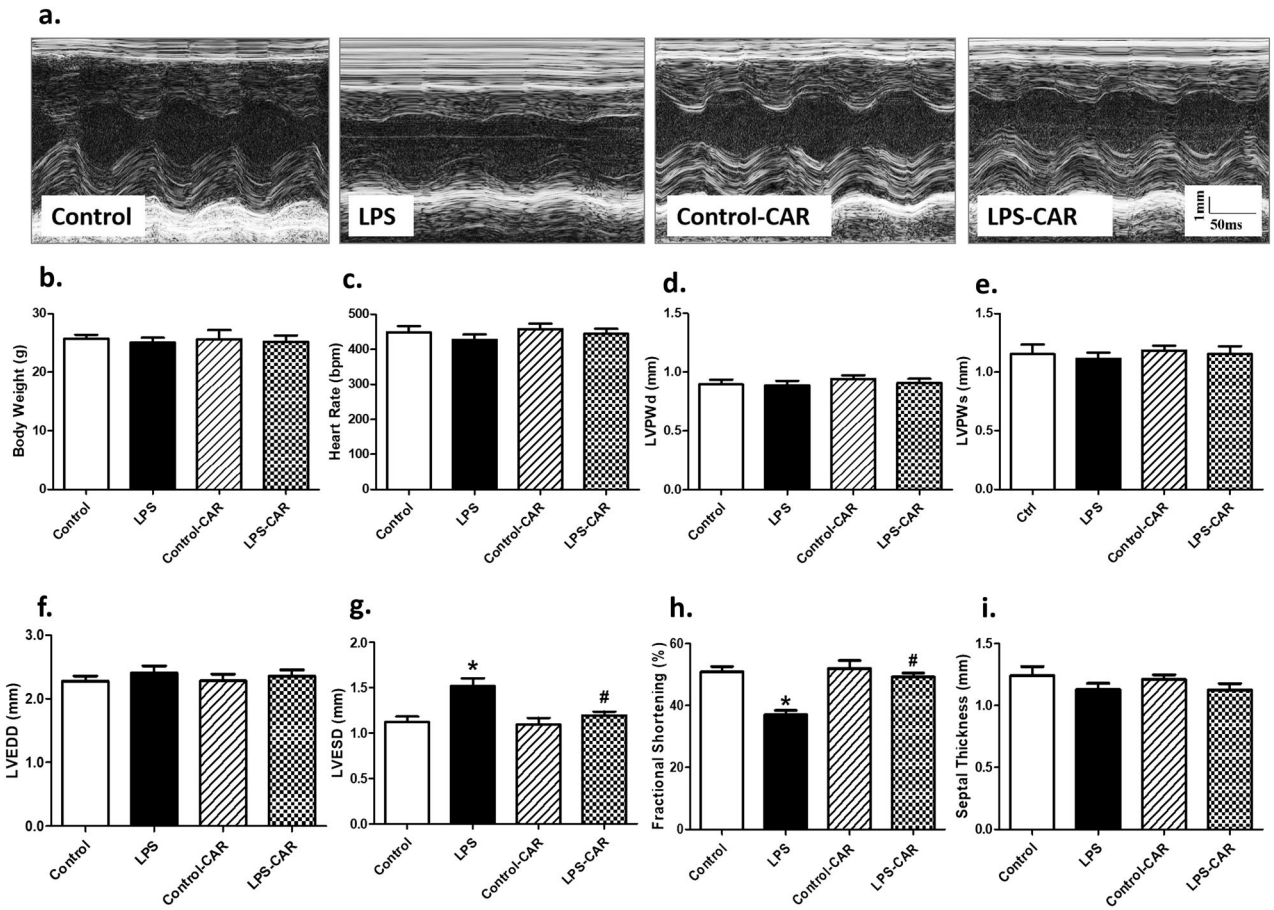

Fig. 1 Effect of CAR treatment (20 mg/kg, p.o.) on LPS challenge (4 mg/kg, i.p., for 6 h)-induced echocardiographic responses. **a** Representative echocardiographic images from all four mouse groups; **b** body weight; **c** heart rate; **d** LV posterior wall thickness in diastole (LVPWd); **e** LV posterior wall thickness in systole (LVPWs); **f** LV end diastolic diameter (LVEDD); **g** LV end systolic diameter (LVESD); **h** fractional shortening; and **i** septal thickness; mean ± SEM; $n = 9$ mice/group, $^{*}P < 0.05$ vs the control group; $^{\#}P < 0.05$ vs the LPS group.

cycles at 95 °C for 10 s and 60 °C for 30 s. Melting curve analysis was performed by increasing the temperature 0.5 °C from 65 to 95 °C for 15 min. The PCR primers were synthesized by Sangon Biotech (Shanghai, China) with primer sequences for SOD1 (forward, 5′-GTCGGCTTCTCGTCTTGCTCTC-3′; reverse, 5′-TTCACCG CTTGCCTTCTGCTC-3′), Gpx1 (forward, 5′-TGGCATTGGCTTGGTGA TTACTGG-3′; reverse, 5′-GGTGGAAAGGCATCGGGAATGG-3′), catalase (forward, 5′-GCTCTCACATGGCTGCGAAGG-3′; reverse, 5′-TCC TCAGGCTCGGCTTCACG-3′), and GAPDH (forward, 5′-GGTTGTCTCC TGCGACTTCA-3′; reverse, 5′-TGGTCCAGGGTTTCTTACTCC-3′). GAP DH was used as a loading control.

Data analysis

Data are shown as the mean ± SEM. Statistical analysis was performed with GraphPad Prism 4.0 software (GraphPad, San Diego, CA) with the significance level set at $P < 0.05$ using multianalysis of variance followed by Tukey's post hoc test.

RESULTS

Effect of CAR on LPS-induced changes in echocardiographic function and morphology

Our results revealed that LPS challenge failed to overtly impact body or heart weights. The echocardiographic examination showed that LPS overtly increased LV end systolic diameter (LVESD), decreased fractional shortening, and had little effect on LV wall thickness, LV end diastolic diameter (LVEDD), and LV mass, consistent with our earlier findings [3, 28]. Although CAR failed to affect the echocardiographic indices tested, it overtly attenuated or nullified the LPS-induced echocardiographic changes. LV wall thickness, LVEDD, LV mass, and heart rate were not overtly affected by LPS challenge, CAR treatment, or both (Fig. 1). Assessment of myocardial morphology using H&E staining or Masson's trichrome staining indicated that neither cardiomyocyte cross-sectional area nor interstitial fibrosis was overtly affected by LPS challenge, CAR treatment, or both (Fig. 2). No remarkable gender difference was noted for either LPS challenge or CAR treatment (data not shown).

CAR nullifies LPS-induced cardiomyocyte contractile defects

In line with the echocardiographic observation, LPS overtly inhibited the mechanical properties of cardiomyocytes, as evidenced by the lower PS and ±dL/dt as well as the prolonged TR_{90}, and led to slight changes in resting cell length and TPS. CAR treatment significantly alleviated LPS-induced cardiomyocyte contractile defects without eliciting any effect itself (Fig. 3).

CAR ameliorates LPS-induced apoptosis and oxidative stress (O_2^- production)

Evaluation of cardiomyocyte apoptosis using TUNEL staining revealed that LPS promoted apoptosis, the effect of which was mitigated by CAR. CAR did not elicit any effect in the control group (Fig. 4). In addition, LPS increased O_2^- production, as evidenced by DHE staining, the effect of which was nullified by

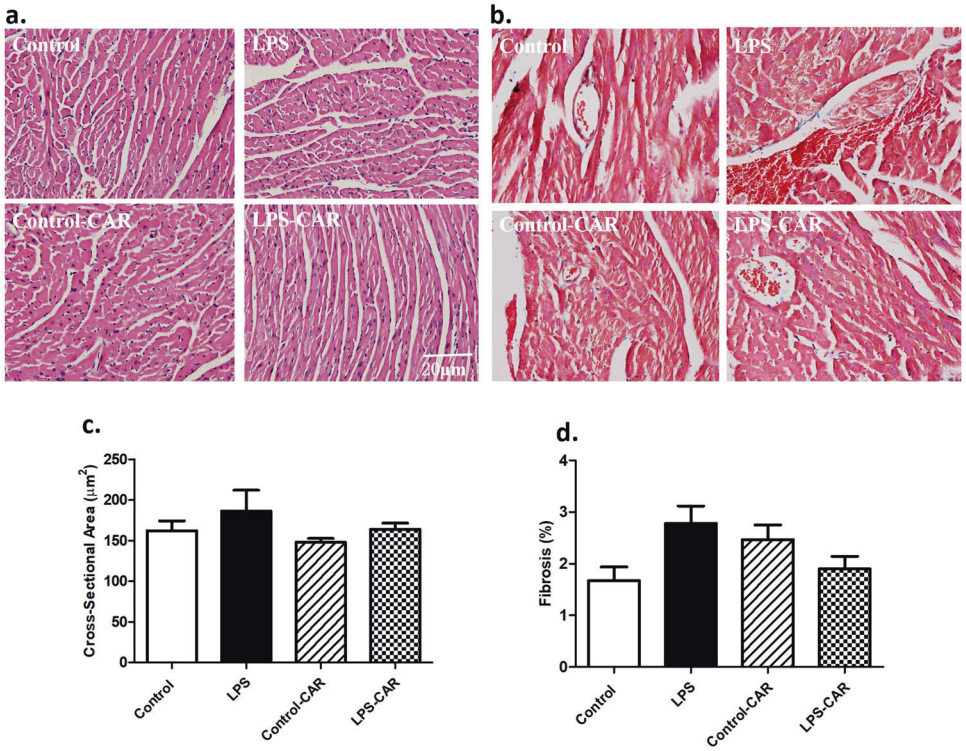

Fig. 2 Effect of CAR treatment (20 mg/kg, p.o.) on LPS challenge (4 mg/kg, i.p., for 6 h)-induced changes in cardiomyocyte cross-sectional area and interstitial fibrosis using H&E and Masson's trichrome staining, respectively. a Representative micrographs depicting H&E staining; **b** representative micrographs depicting Masson's trichrome staining; **c** pooled data of cardiomyocyte cross-sectional area; and **d** pooled data of myocardial fibrosis; mean±SEM; $n = 5$ mice/group.

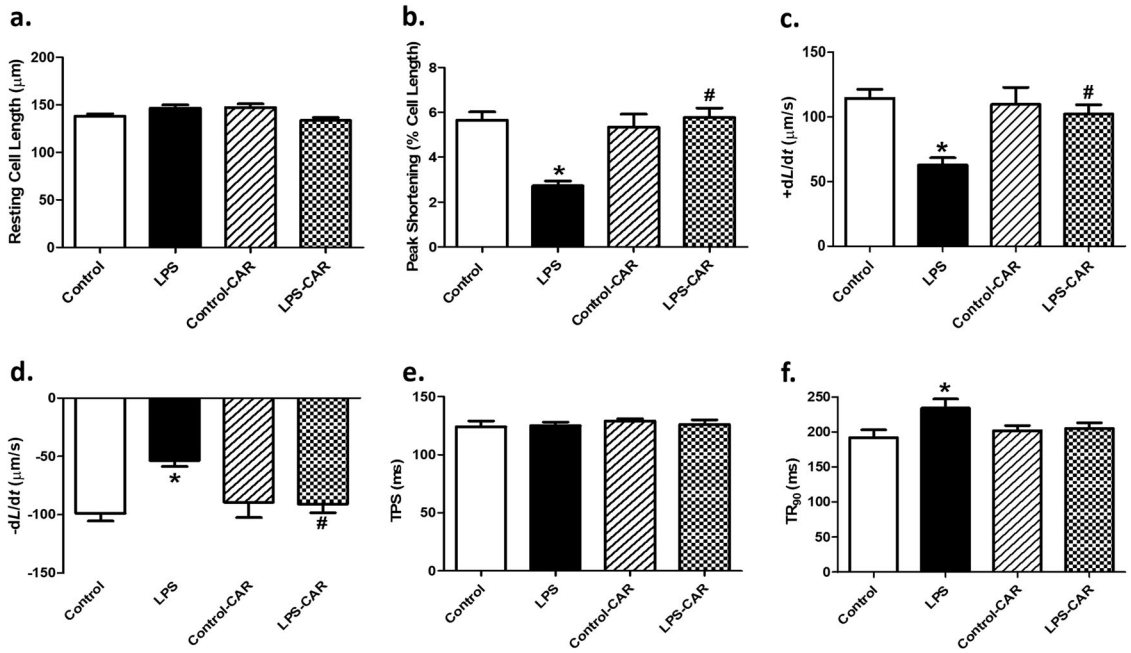

Fig. 3 Effect of CAR treatment (20 mg/kg, p.o.) on LPS challenge (4 mg/kg, i.p., for 6 h)-induced changes in cardiomyocyte contractile properties. a Resting cell length; **b** peak shortening (PS); **c** maximal velocity of shortening ($+dL/dt$); **d** maximal velocity of relengthening ($-dL/dt$); **e** time-to-PS (TPS); and **f** time-to-90% relengthening (TR_{90}). Mean ± SEM, $n = 78–79$ cells from four mice per group. $^{*}P < 0.05$ vs the control group, $^{\#}P < 0.05$ vs the LPS group.

CAR, with little effect from CAR itself (Fig. 5). Further assessment of apoptosis using Western blot analysis suggested that LPS challenge upregulated the protein markers Bax and Caspase-3 as well as downregulated the antiapoptotic protein Bcl-2. Although CAR treatment did not alter the levels of these apoptotic proteins, it ablated the LPS-induced changes in Bax, Caspase-3, and Bcl-2 (Fig. 6a–d). In an effort to consolidate the effect of LPS and CAR on oxidative stress, we evaluated the levels of the

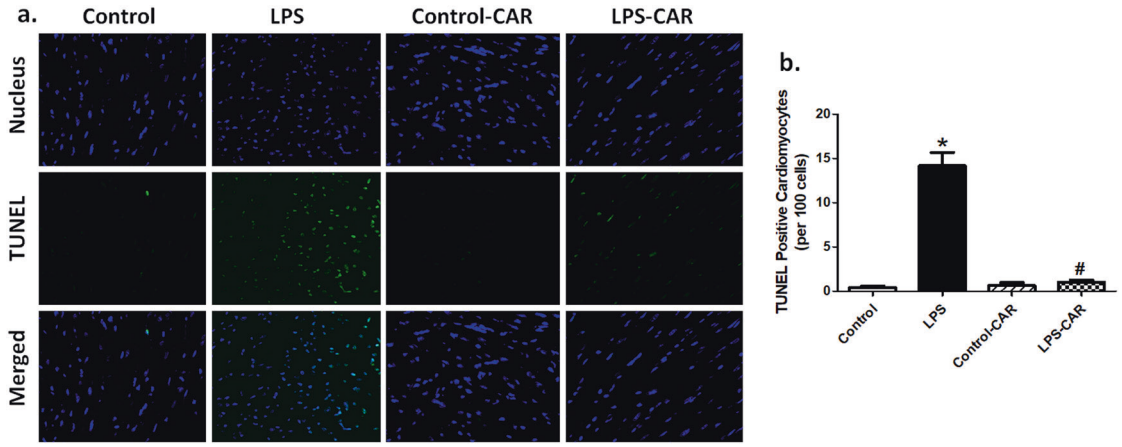

Fig. 4 Effect of CAR treatment (20 mg/kg, p.o.) on LPS challenge (4 mg/kg, i.p., for 6 h)-induced changes in TUNEL apoptosis. **a** Representative images depicting TUNEL-positive nuclei as visualized with fluorescein (green) in the myocardium (×400) from respective mouse groups; **b** quantitative analysis of TUNEL-positive cells (% of total cell number). Mean ± SEM, $n = 17–18$ fields from 5–6 mice per group. $^{*}P < 0.05$ vs the control group, $^{\#}P < 0.05$ vs the LPS group.

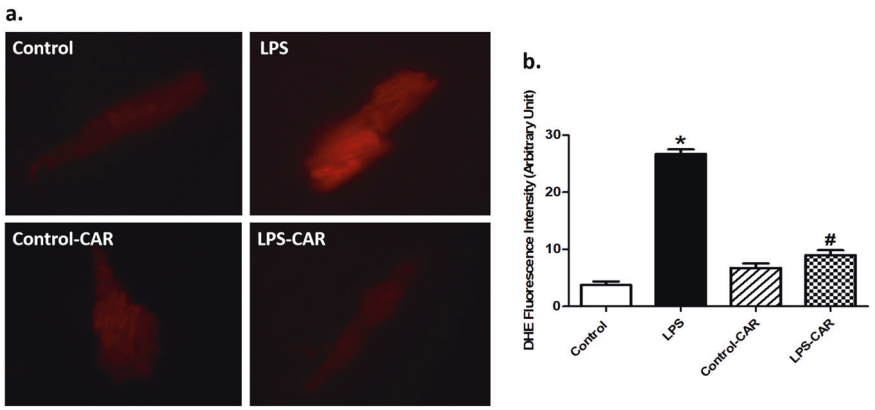

Fig. 5 Effect of CAR treatment (20 mg/kg, p.o.) on LPS challenge (4 mg/kg, i.p., for 6 h)-induced O_2^- production. **a** Representative images depicting cardiomyocyte DHE staining from the respective mouse groups; **b** quantitative analysis of the O_2^- levels. Mean ± SEM, $n = 7$ images from three mice per group, $^{*}P < 0.05$ vs the WT group; $^{\#}P < 0.05$ vs the WT-LPS group.

antioxidants catalase, glutathione peroxidase 1 (GPx1) and Cu-Zn superoxide dismutase (SOD1). Our results revealed that LPS challenge significantly downregulated the levels (protein and mRNA) of catalase, GPx1 and SOD1, and that the effects were nullified by CAR, with little effect from CAR itself (Fig. 6e–k).

CAR ameliorates LPS-induced inflammation, Nrf2 signaling, and NF-κB activation

To determine the possible mechanism(s) underlying the CAR-offered protection against LPS-induced cardiac damage, we evaluated the protein levels of proinflammatory markers. Our data suggested that LPS overtly upregulated the levels of proinflammatory TNF-α, IL-1β, and IL-6, the effects of which were nullified by CAR. CAR did not elicit any effect in the control group (Fig. 7a–d). To determine the possible mechanism behind the LPS- and CAR-induced effects on apoptosis and oxidative stress, the level of the antioxidative transcriptional factor Nrf2 was examined. The data shown in Fig. 7e–g revealed that LPS challenge overtly triggered cytosolic translocation of Nrf2, the effect of which was nullified by CAR, with little effect from CAR itself. Our data further suggested that LPS challenge significantly activated NF-κB phosphorylation (absolute and normalized) without affecting pan NF-κB expression. Although CAR treatment did not affect NF-κB phosphorylation, it ablated LPS-induced NF-κB phosphorylation. Along the same line, LPS challenge overtly increased the phosphorylation of the NF-κB inhibitory IκBα, which prevented the suppression of IκBα on NF-κB phosphorylation. Although CAR treatment did not affect IκBα phosphorylation, it overtly suppressed LPS-induced IκBα phosphorylation, with little effect itself (Fig. 8).

Roles of Nrf2 and NF-κB in the CAR-offered benefits on LPS-induced mechanical defects

An in vitro experiment was conducted to consolidate the cause-effect relationship of Nrf2 and/or NF-κB signaling in LPS- and CAR-elicited cardiomyocyte contractile responses. LPS challenge in vitro significantly decreased PS, $\pm dL/dt$, and prolonged TR_{90} without affecting TPS in cardiomyocytes, the effects of which were nullified by CAR. Interestingly, the beneficial response of CAR was effectively nullified by the Nrf2 inhibitor ML-385 or the NF-κB activator prostratin. Both pharmacological modulators failed to exert any mechanical effects themselves (Fig. 9). These data suggest obligatory roles for Nrf2 and NF-κB in LPS- and CAR-induced cardiac contractile responses.

DISCUSSION

The salient findings from our current study reveal that the medicinal compound CAR effectively protects against LPS-induced cardiac mechanical dysfunction, oxidative stress, inflammation,

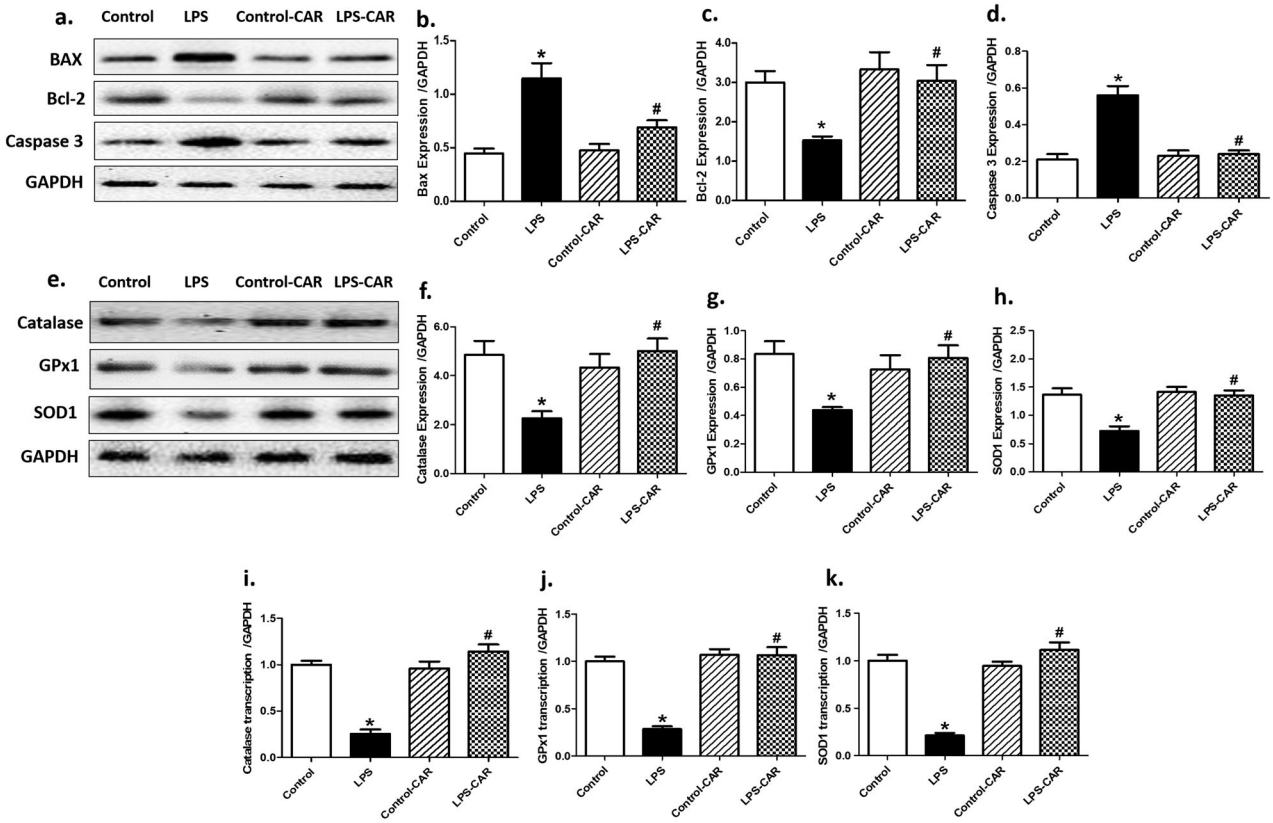

Fig. 6 Effect of CAR treatment (20 mg/kg, p.o.) on LPS challenge (4 mg/kg, i.p., for 6 h)-induced changes in apoptotic and antioxidant proteins and mRNA. a Representative gel blots depicting the levels of BAX, Bcl-2, and Caspase-3 (GAPDH was used as a loading control); **b** BAX levels; **c**: Bcl-2 levels; **d** Caspase-3 levels; **e** representative gel blots depicting the levels of catalase, GPx1 and SOD1 (GAPDH was used as a loading control); **f** catalase protein levels; **g** GPx1 protein levels; **h** SOD1 protein levels. **h** catalase transcription levels; **i** GPx1 transcription levels; and **j** SOD1 transcription levels. Mean ± SEM, $n = 5$–9 mice per group, $^{*}P < 0.05$ vs the control group, $^{\#}P < 0.05$ vs the LPS group.

and apoptosis. These findings are in line with notion reported in earlier reports with regard to the anti-inflammatory and antioxidant properties of CAR [17–19]. Moreover, our findings support the previously reported benefits of CAR in LPS-induced septic lung injury through inhibition of inflammation and endothelial barrier dysfunction [20, 21]. Taken together, our findings depict a favorable role for CAR in therapy against LPS-induced cardiac contractile anomalies.

Unfavorable changes are evident in endotoxemic hearts, as manifested by reduced cardiac contractile function [4, 39–41]. In our current experimental setting, LPS compromised myocardial contractile function, as evidenced by poor fractional shortening, enlarged LVESD, and decreased cardiomyocyte contractile capacity with unchanged LVEDD, heart rate, LV wall thickness, cardiomyocyte cross-sectional area, and myocardial fibrosis. The lack of change in cardiac morphology (i.e., cross-sectional area and fibrosis) may be simply due to the relatively short duration of LPS challenge (6 h). These LPS-induced detrimental functional alterations in the heart are consistent with pronounced apoptosis (Bax, Bcl-2, and cleaved Caspase-3), compromised antioxidant defense (both the protein and mRNA levels of catalase, GPx1 and SOD1), O_2^- accumulation and inflammation (IL-1β, IL-6, and TNF-α) in septic hearts. Interestingly, CAR treatment is capable of countering LPS-induced mechanical anomalies and oxidative stress (e.g., intracellular O_2^-, antioxidant enzymes SOD1, catalase, and GPx1, as well as proapoptotic Bax and cleaved Caspase-3 and antiapoptotic Bcl-2). These findings support likely roles for oxidative stress and antioxidant defense in the CAR-offered beneficial mechanical and apoptotic responses in the face of LPS challenge.

Similar to our earlier report [13], data from our present study revealed overt inflammatory, apoptotic, and prooxidant responses in LPS-challenged hearts. In our hands, LPS challenge overtly upregulated the levels of IL-1β and IL-6, the effects of which were negated by CAR. These observations are in line with our earlier report with regard to the benefit of the anti-inflammation maneuver in septic cardiomyopathy [4, 25], in accordance with our reported improved mechanical and apoptotic profiles in LPS-challenged mice treated with CAR. LPS is perceived to turn on innate immune responses to release proinflammatory cytokines (e.g., interleukins) [42, 43]. Our current findings suggest that CAR may suppress cardiac cardiomyopathy triggered by sepsis, possibly by mitigating the inflammatory response and oxidative stress. The anti-inflammatory and antioxidant mechanisms of CAR (at both the protein and mRNA levels) might be related to the induction of heme oxygenase-1 (HO-1) expression and the inhibition of the NLRP3 inflammasome, iNOS expression, and the NF-κB and mitogen-activated protein kinase signaling cascades [17, 21]. These findings favor a concerted therapeutic benefit of CAR in the management of multiple stresses in the septic heart.

The transcription factor NF-κB functions as an essential factor in the regulation of inflammatory mediators and is activated by phosphorylation of NF-κB inhibitory IκBα. NF-κB closely regulates the production of proinflammatory cytokines. As another essential regulator of inflammation and oxidative responses, Nrf2 increases the levels of antioxidants and cytoprotective genes, triggering an anti-inflammatory defense profile in an effort to restore oxidative homeostasis [44]. Nrf2 is known to inhibit the activation of proinflammatory genes [45], consistent with findings from our current study. Nrf2 has been shown to protect against chronic

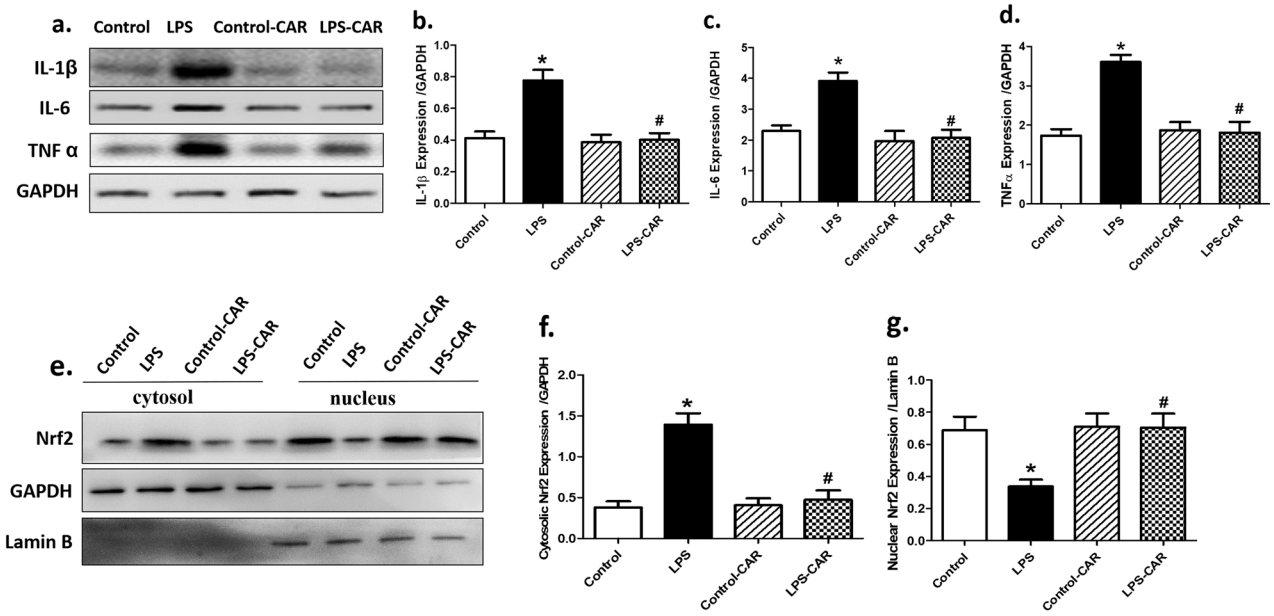

Fig. 7 Effect of CAR treatment (20 mg/kg, p.o.) on LPS challenge (4 mg/kg, i.p., for 6 h)-induced changes in proinflammatory proteins and Nrf2 nuclear translocation. a Representative gel blots depicting the levels of proinflammatory markers, including IL-1β, IL-6, TNF-α, as well as cytosolic and nuclear Nrf2 (GAPDH was used as a loading control, with Lamin B used as loading control for the nucleus); **b** IL-1β; **c** IL-6; **d** TNF-α; **e** cytosolic Nrf2 levels; and **f** nuclear Nrf2 levels. Mean ± SEM, $n = 5–7$ mice per group, $^{*}P < 0.05$ vs the control group; $^{\#}P < 0.05$ vs the LPS group.

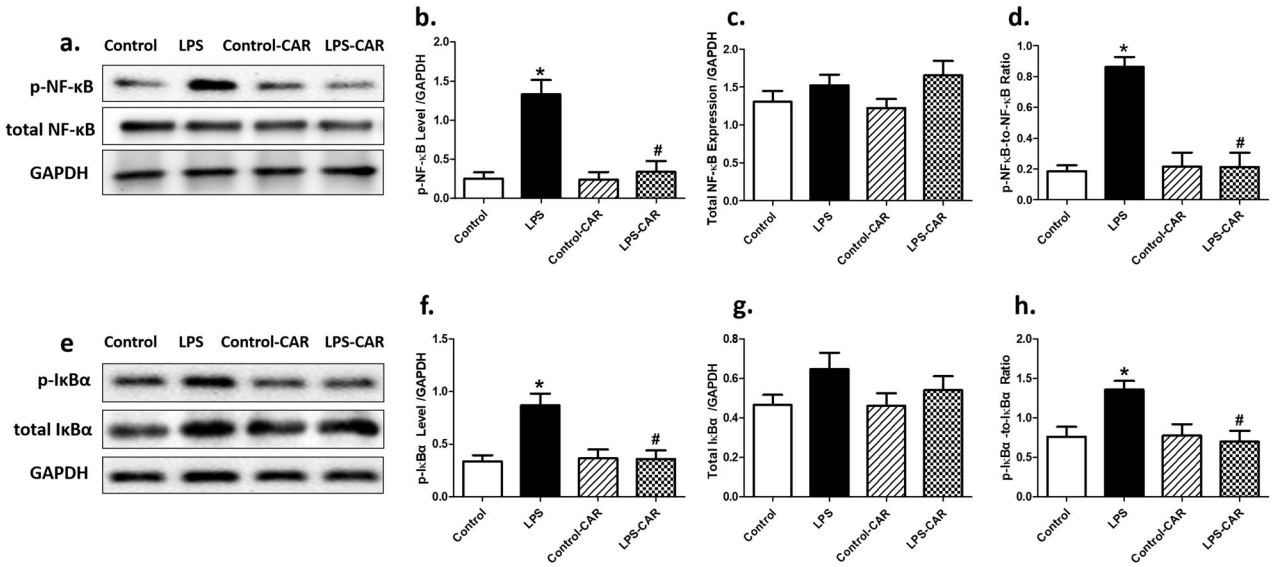

Fig. 8 Effect of CAR treatment (20 mg/kg, p.o.) on LPS challenge (4 mg/kg, i.p., for 6 h)-induced changes in phosphorylation of NF-κB and IκBα. a Representative blots depicting the levels of pan and phosphorylated NF-κB (GAPDH as loading control); **b** pNF-κB levels; **c** NF-κB levels; **d** pNF-κB-to-NF-κB ratio; **e** representative blots depicting the levels of pan and phosphorylated IκBα (GAPDH as loading control); **f** pIκBα levels; **g** IκBα levels; and **h** pIκBα-to-IκBα ratio. Mean ± SEM, $n = 5–7$ mice per group, $^{*}P < 0.05$ vs the control group; $^{\#}P < 0.05$ vs the LPS group.

pathological conditions, such as cardiovascular and neurodegenerative diseases [46, 47]. Our present experimental findings showed increased cytosolic translocation of Nrf2, the effect of which was abolished by CAR, denoting a likely role for Nrf2 translocation in the CAR-offered cardiac benefit against septic cardiomyopathy. De novo synthesized Nrf2 is stabilized in the nucleus and induces the expression of cytoprotective target genes to execute its beneficial roles in detoxification, antioxidation, and metabolism [48]. To this end, activation of the Nrf2 pathway and inhibition of NF-κB might represent a promising strategy for the management of septic cardiomyopathy. This speculation received support from an in vitro mechanical study in which the inhibition of Nrf2 using ML-385 and the activation of NF-κB using prostratin nullified the CAR-offered benefits against LPS-induced cardiomyocyte anomalies. ML-385, a specific Nrf2 inhibitor, suppresses Nrf2 transcriptional activity through binding to Neh1, the Cap 'N' Collar Basic Leucine Zipper domain of Nrf2, thus interfering with the binding of the V-Maf Avian Musculoaponeurotic Fibrosarcoma Oncogene Homolog G-NRF2 protein complex to regulatory DNA sequences [49]. Prostratin, a nontumorigenic phorbol ester, promotes phosphorylation and degradation of the NF-κB inhibitor IκBα and increases the level of deubiquitinase A20, a negative

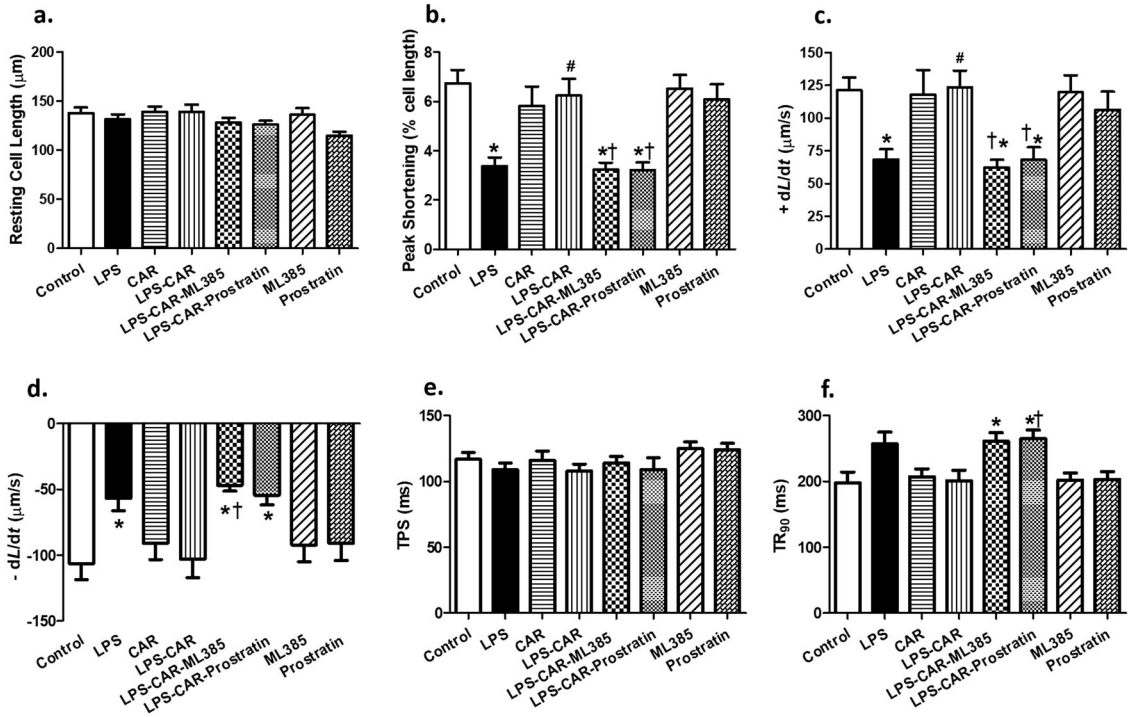

Fig. 9 Role of Nrf2 and NF-κB signals in CAR-offered protection against LPS-induced cardiomyocyte contractile dysfunction. Mouse cardiomyocytes from adult C57BL/6 mice were exposed to LPS (4 μg/mL) for 6 h in the absence or presence of CAR (10 μM), the Nrf2 inhibitor ML-385 (20 μM), or the NF-κB activator prostratin (2 μM). **a** resting cell length; **b** peak shortening (PS); **c** maximal velocity of shortening (+d*L*/d*t*); **d** maximal velocity of relengthening (−d*L*/d*t*); **e** time-to-peak shortening (TPS); and **f** time-to-90% relengthening (TR_{90}). Mean ± SEM, $n =$ 30 cells from three mice per group, $^{*}P < 0.05$ vs the control group, $^{\#}P < 0.05$ vs the LPS group, $^{\dagger}P < 0.05$ vs the LPS-CAR group.

feedback regulator in NF-κB signaling [34]. These findings suggest a role for the Nrf2-NF-κB signaling cascade in the governance of inflammation and oxidative stress in septic cardiomyopathy. It may be speculated that CAR attenuates the phosphorylation of NF-κB and cytosolic translocation of the transcriptional factor Nrf2, leading to suppression of proinflammatory cytokines (TNF-α, IL-1β, and IL-6) and increased expression of antioxidants, including catalase, GPx1 and SOD1 (protein and mRNA levels).

The Keap1/Nrf2-antioxidant response element (ARE) signaling cascade participates in oxidative stress and inflammation and serves as a novel pharmacological target for many chronic diseases, including cardiovascular and inflammatory bowel diseases [50, 51]. Natural and synthetic compounds may both regulate the Keap1/Nrf2-ARE signaling cascade [52]. Nrf2 is typically activated by electrophilic activators (modifications of Keap1 cysteine residues) or nonelectrophilic activators (the protein–protein interface of Keap1/Nrf2) [52, 53]. A number of compounds, including heavy metals, phenols, and ROS, may turn on Nrf2 [54]. CDDO-Im (the imidazolide derivative of the triterpenoid CDDO) is one of the most potent Nrf2 activators at nanomolar concentrations. However, CDDO-Im may activate additional signals at micromolar levels [55, 56]. The regulation of Nrf2 by CDDO-Im is also cell type dependent. CDDO-Im inhibits NF-κB DNA binding and early IFNγ and TNF-α production in an Nrf2-dependent manner [57]. Although CDDO-Im and CAR have been shown to turn on Nrf2 through the modification of essential cysteine residues on Keap1, they exhibit distinct potency differences (e.g., 10–100 μM CAR vs 0.001–0.1 μM CDDO-Im employed in respective experiments) [57, 58]. In addition, CAR not only inhibits Nrf2 degradation by reducing Keap1 levels but also increases Nrf2 levels, both of which facilitate the activation of Nrf2-ARE signaling [58]. Data from our study suggest that CAR may promote the nuclear translocation of Nrf2, along with increased antioxidant defense (catalase, GPx1 and SOD1). These findings are in line with a previous study in which the treatment of PC12 cells with CAR promoted Nrf2 nuclear translocation and upregulated the levels of GSH, HO-1, NQO1, Trx1, TrxR1, GCLC, and glutamate-cysteine ligase modifier (GCLM) [59]. These authors also revealed that Nrf2 knockdown abolished the neuroprotective effects of CAR, indicating an obligatory role for Nrf2 in CAR-evoked neuroprotection [59]. Along the same line, CAR drastically inhibited oxidative stress, apoptosis, and the inflammatory response in doxorubicin-challenged hearts by activating the Nrf2-related cytoprotective system, eventually improving cardiac function [58].

In summary, the salient findings from our study suggest that CAR effectively rescues LPS-induced cardiac injury through an Nrf2-NF-κB-mediated mechanism. These findings should allow a better understanding of the therapeutic value of CAR in the management of septic cardiomyopathy. CAR is expected to protect against LPS-induced cardiac anomalies through activation of Nrf2 and suppression of NF-κB-mediated oxidative stress and apoptosis, en route to the alleviation of septic cardiac dysfunction. The findings of this study indicate the therapeutic value of CAR for treating endotoxemia-induced cardiac anomalies.

ACKNOWLEDGEMENTS

This work was supported in part by the National Natural Science Foundation of China (81671938, 81571895).

AUTHOR CONTRIBUTIONS

YT, HHW, MMS, WJZ, MLD, and WG performed the experimental study; JR, MLD, and HP conceived and designed the study and drafted, edited and approved the paper.

ADDITIONAL INFORMATION

Competing interests: The authors declare no competing interests.

REFERENCES

1. Arfaras-Melainis A, Polyzogopoulou E, Triposkiadis F, Xanthopoulos A, Ikonomidis I, Mebazaa A, et al. Heart failure and sepsis: practical recommendations for the optimal management. Heart Fail Rev. 2020;25:183–94.
2. Ceylan-Isik AF, Zhao P, Zhang B, Xiao X, Su G, Ren J. Cardiac overexpression of metallothionein rescues cardiac contractile dysfunction and endoplasmic reticulum stress but not autophagy in sepsis. J Mol Cell Cardiol. 2010;48:367–78.
3. Turdi S, Han X, Huff AF, Roe ND, Hu N, Gao F, et al. Cardiac-specific overexpression of catalase attenuates lipopolysaccharide-induced myocardial contractile dysfunction: role of autophagy. Free Radic Biol Med. 2012;53:1327–38.
4. Zhang Y, Xu X, Ceylan-Isik AF, Dong M, Pei Z, Li Y, et al. Ablation of Akt2 protects against lipopolysaccharide-induced cardiac dysfunction: role of Akt ubiquitination E3 ligase TRAF6. J Mol Cell Cardiol. 2014;74:76–87.
5. Coverstone ED, Bach RG, Chen L, Bierut LJ, Li AY, Lenzini PA, et al. A novel genetic marker of decreased inflammation and improved survival after acute myocardial infarction. Basic Res Cardiol. 2018;113:38.
6. Charpentier J, Luyt CE, Fulla Y, Vinsonneau C, Cariou A, Grabar S, et al. Brain natriuretic peptide: a marker of myocardial dysfunction and prognosis during severe sepsis. Crit Care Med. 2004;32:660–5.
7. Ren J, Wu S. A burning issue: do sepsis and systemic inflammatory response syndrome (SIRS) directly contribute to cardiac dysfunction? Front Biosci. 2006;11:15–22.
8. Stanzani G, Duchen MR, Singer M. The role of mitochondria in sepsis-induced cardiomyopathy. Biochim Biophys Acta Mol Basis Dis. 2019;1865:759–73.
9. Tan Y, Chen S, Zhong J, Ren J, Dong M. Mitochondrial injury and targeted intervention in septic cardiomyopathy. Curr Pharmacol Des. 2019;25:2060–70.
10. Durand A, Duburcq T, Dekeyser T, Neviere R, Howsam M, Favory R, et al. Involvement of mitochondrial disorders in septic cardiomyopathy. Oxid Med Cell Longev. 2017;2017:4076348.
11. Soriano FG, Lorigados CB, Pacher P, Szabo C. Effects of a potent peroxynitrite decomposition catalyst in murine models of endotoxemia and sepsis. Shock. 2011;35:560–6.
12. Torres-Duenas D, Celes MR, Freitas A, Alves-Filho JC, Spiller F, Dal-Secco D, et al. Peroxynitrite mediates the failure of neutrophil migration in severe polymicrobial sepsis in mice. Br J Pharmacol. 2007;152:341–52.
13. Pang J, Peng H, Wang S, Xu X, Xu F, Wang Q, et al. Mitochondrial ALDH2 protects against lipopolysaccharide-induced myocardial contractile dysfunction by suppression of ER stress and autophagy. Biochim Biophys Acta Mol Basis Dis. 2019;1865:1627–41.
14. Mahmoud AM, Hernandez Bautista RJ, Sandhu MA, Hussein OE. Beneficial effects of citrus flavonoids on cardiovascular and metabolic health. Oxid Med Cell Longev. 2019;2019:5484138.
15. Fan XJ, Ren J. Compensation: a contemporary regulatory machinery in cardiovascular diseases? Cardiovasc Toxicol. 2012;12:275–84.
16. Fan XJ, Yu H, Ren J. Homeostasis and compensatory homeostasis: bridging western medicine and traditional chinese medicine. Curr Cardiol Rev. 2011;7:43–6.
17. Li YY, Huang SS, Lee MM, Deng JS, Huang GJ. Anti-inflammatory activities of cardamonin from *Alpinia katsumadai* through heme oxygenase-1 induction and inhibition of NF-kappaB and MAPK signaling pathway in the carrageenan-induced paw edema. Int Immunopharmacol. 2015;25:332–9.
18. Peng S, Hou Y, Yao J, Fang J. Activation of Nrf2-driven antioxidant enzymes by cardamonin confers neuroprotection of PC12 cells against oxidative damage. Food Funct. 2017;8:997–1007.
19. Jantan I, Raweh SM, Sirat HM, Jamil S, Mohd Yasin YH, Jalil J, et al. Inhibitory effect of compounds from Zingiberaceae species on human platelet aggregation. Phytomedicine. 2008;15:306–9.
20. Wei Z, Yang J, Xia YF, Huang WZ, Wang ZT, Dai Y. Cardamonin protects septic mice from acute lung injury by preventing endothelial barrier dysfunction. J Biochem Mol Toxicol. 2012;26:282–90.
21. Wang Z, Xu G, Gao Y, Zhan X, Qin N, Fu S, et al. Cardamonin from a medicinal herb protects against LPS-induced septic shock by suppressing NLRP3 inflammasome. Acta Pharm Sin B. 2019;9:734–44.
22. Li W, Wu X, Li M, Wang Z, Li B, Qu X, et al. Cardamonin alleviates pressure overload-induced cardiac remodeling and dysfunction through inhibition of oxidative stress. J Cardiovasc Pharmacol. 2016;68:441–51.
23. Israf DA, Khaizurin TA, Syahida A, Lajis NH, Khozirah S. Cardamonin inhibits COX and iNOS expression via inhibition of p65NF-kappaB nuclear translocation and Ikappa-B phosphorylation in RAW 264.7 macrophage cells. Mol Immunol. 2007;44:673–9.
24. Lee M-Y, Seo C-S, Lee J-A, Shin I-S, Kim S-J, Ha H, et al. *Alpinia katsumadai* HAYATA seed extract inhibit LPS-induced inflammation by induction of heme oxygenase-1 in RAW264.7. Cells. 2012;35:746–57.
25. Ren J, Xu X, Wang Q, Ren SY, Dong M, Zhang Y. Permissive role of AMPK and autophagy in adiponectin deficiency-accentuated myocardial injury and inflammation in endotoxemia. J Mol Cell Cardiol. 2016;93:18–31.
26. Sun Y, Cai Y, Zang QS. Cardiac autophagy in sepsis. Cells. 2019;8:141.
27. Sun Y, Yao X, Zhang QJ, Zhu M, Liu ZP, Ci B, et al. Beclin-1-dependent autophagy protects the heart during sepsis. Circulation. 2018;138:2247–62.
28. Dong M, Hu N, Hua Y, Xu X, Kandadi MR, Guo R, et al. Chronic Akt activation attenuated lipopolysaccharide-induced cardiac dysfunction via Akt/GSK3beta-dependent inhibition of apoptosis and ER stress. Biochim Biophys Acta. 2013;1832:848–63.
29. Koentges C, Cimolai MC, Pfeil K, Wolf D, Marchini T, Tarkhnishvili A, et al. Impaired SIRT3 activity mediates cardiac dysfunction in endotoxemia by calpain-dependent disruption of ATP synthesis. J Mol Cell Cardiol. 2019;133:138–47.
30. Wang S, Zhu X, Xiong L, Ren J. Ablation of Akt2 prevents paraquat-induced myocardial mitochondrial injury and contractile dysfunction: role of Nrf2. Toxicol Lett. 2017;269:1–14.
31. Ceylan AF, Wang S, Kandadi MR, Chen J, Hua Y, Pei Z, et al. Cardiomyocyte-specific knockout of endothelin receptor a attenuates obesity cardiomyopathy. Biochim Biophys Acta Mol Basis Dis. 2018;1864:3339–52.
32. Li SY, Gilbert SA, Li Q, Ren J. Aldehyde dehydrogenase-2 (ALDH2) ameliorates chronic alcohol ingestion-induced myocardial insulin resistance and endoplasmic reticulum stress. J Mol Cell Cardiol. 2009;47:247–55.
33. Li D, Qi J, Wang J, Pan Y, Li J, Xia X, et al. Protective effect of dihydroartemisinin in inhibiting senescence of myeloid-derived suppressor cells from lupus mice via Nrf2/HO-1 pathway. Free Radic Biol Med. 2019;143:260–74.
34. Chen D, Wang H, Aweya JJ, Chen Y, Chen M, Wu X, et al. HMBA enhances prostratin-induced activation of latent HIV-1 via suppressing the expression of negative feedback regulator A20/TNFAIP3 in NF-kappaB signaling. Biomed Res Int. 2016;2016:5173205.
35. Wang Z, Zhang Y, Guo J, Jin K, Li J, Guo X, et al. Inhibition of protein kinase C betaII isoform rescues glucose toxicity-induced cardiomyocyte contractile dysfunction: role of mitochondria. Life Sci. 2013;93:116–24.
36. Zhang Y, Xia Z, La Cour KH, Ren J. Activation of Akt rescues endoplasmic reticulum stress-impaired murine cardiac contractile function via glycogen synthase kinase-3beta-mediated suppression of mitochondrial permeation pore opening. Antioxid Redox Signal. 2011;15:2407–24.
37. Hasna J, Hague F, Rodat-Despoix L, Geerts D, Leroy C, Tulasne D, et al. Orai3 calcium channel and resistance to chemotherapy in breast cancer cells: the p53 connection. Cell Death Differ. 2018;25:693–707.
38. Wei Y, Chang Y, Zeng H, Liu G, He C, Shi H. RAV transcription factors are essential for disease resistance against cassava bacterial blight via activation of melatonin biosynthesis genes. J Pineal Res. 2018;64:10.
39. Ren J, Ren BH, Sharma AC. Sepsis-induced depressed contractile function of isolated ventricular myocytes is due to altered calcium transient properties. Shock. 2002;18:285–8.
40. Lew WY, Bayna E, Dalle Molle E, Contu R, Condorelli G, Tang T. Myocardial fibrosis induced by exposure to subclinical lipopolysaccharide is associated with decreased miR-29c and enhanced NOX2 expression in mice. PLoS ONE. 2014;9:e107556.
41. Lew WY, Bayna E, Molle ED, Dalton ND, Lai NC, Bhargava V, et al. Recurrent exposure to subclinical lipopolysaccharide increases mortality and induces cardiac fibrosis in mice. PLoS ONE. 2013;8:e61057.
42. Gasteiger G, D'Osualdo A, Schubert DA, Weber A, Bruscia EM, Hartl D. Cellular innate immunity: an old game with new players. J Innate Immun. 2017;9:111–25.
43. Guo S, Nighot M, Al-Sadi R, Alhmoud T, Nighot P, Ma TY. Lipopolysaccharide regulation of intestinal tight junction permeability is mediated by TLR4 signal transduction pathway activation of FAK and MyD88. J Immunol. 2015;195:4999–5010.
44. Vomund S, Schafer A, Parnham MJ, Brune B, von Knethen A. Nrf2, the master regulator of anti-oxidative responses. Int J Mol Sci. 2017;18:E2772.
45. Kobayashi EH, Suzuki T, Funayama R, Nagashima T, Hayashi M, Sekine H, et al. Nrf2 suppresses macrophage inflammatory response by blocking proinflammatory cytokine transcription. Nat Commun. 2016;7:11624.
46. Li J, Zhang C, Xing Y, Janicki JS, Yamamoto M, Wang XL, et al. Up-regulation of p27(kip1) contributes to Nrf2-mediated protection against angiotensin II-induced cardiac hypertrophy. Cardiovascular Res. 2011;90:315–24.
47. Biswal S, Thimmulappa RK, Harvey CJ. Experimental therapeutics of Nrf2 as a target for prevention of bacterial exacerbations in COPD. Proc Am Thorac Soc. 2012;9:47–51.
48. Walsh J, Jenkins RE, Wong M, Olayanju A, Powell H, Copple I, et al. Identification and quantification of the basal and inducible Nrf2-dependent proteomes in mouse liver: biochemical, pharmacological and toxicological implications. J Proteom. 2014;108:171–87.
49. Singh A, Venkannagari S, Oh KH, Zhang YQ, Rohde JM, Liu L, et al. Small molecule inhibitor of NRF2 selectively intervenes therapeutic resistance in KEAP1-Deficient NSCLC tumors. ACS Chem Biol. 2016;11:3214–25.
50. Cuadrado A, Manda G, Hassan A, Alcaraz MJ, Barbas C, Daiber A, et al. Transcription factor NRF2 as a therapeutic target for chronic diseases: a systems medicine approach. Pharmacol Rev. 2018;70:348–83.

51. Lu MC, Ji JA, Jiang ZY, You QD. The Keap1-Nrf2-ARE pathway as a potential preventive and therapeutic target: an update. Med Res Rev. 2016;36:924–63.
52. de Freitas Silva M, Pruccoli L, Morroni F, Sita G, Seghetti F, Viegas C, et al. The Keap1/Nrf2-ARE pathway as a pharmacological target for chalcones. Molecules. 2018;23:E1803.
53. Abed DA, Goldstein M, Albanyan H, Jin H, Hu L. Discovery of direct inhibitors of Keap1-Nrf2 protein–protein interaction as potential therapeutic and preventive agents. Acta Pharm Sin B. 2015;5:285–99.
54. Kensler TW, Wakabayashi N, Biswal S. Cell survival responses to environmental stresses via the Keap1-Nrf2-ARE pathway. Annu Rev Pharmacol Toxicol. 2007;47:89–116.
55. Dinkova-Kostova AT, Liby K, Stephenson KK, Holtzclaw WD, Gao X, Suh N, et al. Extremely potent triterpenoid inducers of the phase 2 response: correlations of protection against oxidant and inflammatory stress. Proc Natl Acad Sci USA. 2005;102:4584–9.
56. Liby KT, Sporn MB. Synthetic oleanane triterpenoids: multifunctional drugs with a broad range of applications for prevention and treatment of chronic disease. Pharmacol Rev. 2012;64:972–1003.
57. Zagorski JW, Turley AE, Freeborn RA, VanDenBerg KR, Dover HE, Kardell BR, et al. Differential effects of the Nrf2 activators tBHQ and CDDO-Im on the early events of T cell activation. Biochem Pharmacol. 2018;147:67–76.
58. Qi W, Boliang W, Xiaoxi T, Guoqiang F, Jianbo X, Gang W. Cardamonin protects against doxorubicin-induced cardiotoxicity in mice by restraining oxidative stress and inflammation associated with Nrf2 signaling. Biomed Pharmacother. 2020;122:109547.
59. De Spirt S, Eckers A, Wehrend C, Micoogullari M, Sies H, Stahl W, et al. Interplay between the chalcone cardamonin and selenium in the biosynthesis of Nrf2-regulated antioxidant enzymes in intestinal Caco-2 cells. Free Radic Biol Med. 2016;91:164–71.